

Supporting Information:

A highly stable face-extended diamondoid cluster-organic framework incorporating infinite inorganic guests

Wei-Hui Fang,^a Lei Zhang,^a Jian Zhang,^a and Guo-Yu Yang^{*ab}

^aState Key Laboratory of Structural Chemistry, Fujian Institute of Research on the Structure of Matter, Chinese Academy of Sciences, Fuzhou, Fujian 350002, China

^bMOE Key Laboratory of Cluster Science, School of Chemistry, Beijing Institute of Technology, Beijing 100081, China

Corresponding Author

*E-mail: ygy@fjirsm.ac.cn; ygy@bit.edu.cn

Content

Experimental Section:	2
Materials and physical measurements.....	2
X-Ray Crystallography	2
Supporting Figures:	2
Fig. S1 The asymmetric unit of complex 1	3
Fig. S2 The perspective view of the Cu ₄ O tetrahedron.	3
Fig. S3 The topological representation of the three-fold interpenetrating dia net of complex 1	3
Fig. S4 The interlocked adamantane units of three independent diamond-like nets.	4
Fig. S5 The scheme representation of the 1D copper halide chains inset in a adamantane unit (left) and the overall side view of the compound 1 (right).	4
Fig. S6 The H-bonding interactions between host framework and guest chains.....	4
Fig. S7 The TGA curves of the compound 1	5
Fig. S8 The bands gap of the compound 1	5
Fig. S9 PXRD patterns of 1 after being soaked in water and exposed in air for months.	5
Fig. S10 Illustration of the “rhombus grid” showing the crystal structure transformation.....	6
Fig. S11 The simulated and experimental PXRD patterns of compound 1	6
Fig. S12 The IR spectra of the complex 1	6
Supporting Tables:	7
Table S1 A summary of interpenetrating <i>dia</i> nets assembled by L ligands	7
Table S2 The Bond valence sum (BVS) analysis.....	7
Table S3 Hydrogen bond lengths (Å) and bond angles (°) for compound 1	8
Table S4 Temperature dependence of the unit-cell parameters of compound 1	8
Table S5 Crystal data and structural refinement results.....	8
Table S6 Coordination bond lengths and angles of 1	9
References	10

Experimental Section:

Materials and physical measurements. All chemicals and solvents were commercially purchased and used without further purification. Elemental analysis was measured on a Vario MICRO Elemental Analyzer instrument. IR spectra (KBr pellets) were recorded on an ABB Bomem MB102 spectrometer over a range 400-4000 cm⁻¹. The thermogravimetric analyses (TGA) were performed on a Mettler Toledo TGA/SDTA 851^e analyzer in air atmosphere with a heating rate of 10 °C/min from 30 °C to 1000 °C. Powder X-ray diffraction (PXRD) data were collected on a Rigaku Mini Flex II diffractometer using CuK α radiation ($\lambda = 1.54056\text{\AA}$) under ambient conditions. The UV diffuse reflection data were recorded at room temperature using a powder sample with BaSO₄ as a standard (100% reflectance) on a PerkinElmer Lamda-950 UV spectrophotometer and scanned at 200-800 nm. The absorption data are calculated from the Kubelka-Munk function, $(F(R)=(1-R)^2/2R)$,¹ where R representing the reflectance, K the absorption, and S the scattering. Transmission electron microscopy (TEM) images and high-resolution transmission electron microscopy (HRTEM) images were obtained on a Tecnai G2 F20 field emission transmission electron microscope at an accelerating voltage of 200 kV. The powder sample was dispersed in ethanol and a drop of the slurry was placed onto a TEM grid.

X-Ray Crystallography. Crystallographic data of complexes **1** were collected on a Supernova single crystal diffractometer equipped with graphite-monochromatic CuK α radiation ($\lambda = 1.54178 \text{\AA}$) at 100 K and 298 K. The test temperature was controlled by dry N₂ flow using a Cryo Stream 700 system (Agilent Technologies, USA), and corrected by a thermal couple at the crystal position. The variable temperature unit-cell parameters were obtained by indexing the diffraction spots that were obtained with diffraction images. The structure was solved with direct methods using SHELXS-97² and refined with the full-matrix least-squares technique based on F^2 using the SHELXL-97.³ Non-hydrogen atoms were refined anisotropically, and all hydrogen atoms bond C were generated geometrically. Crystallographic diagrams were drawn using the DIAMOND software package.⁴

Supporting Fig.s:

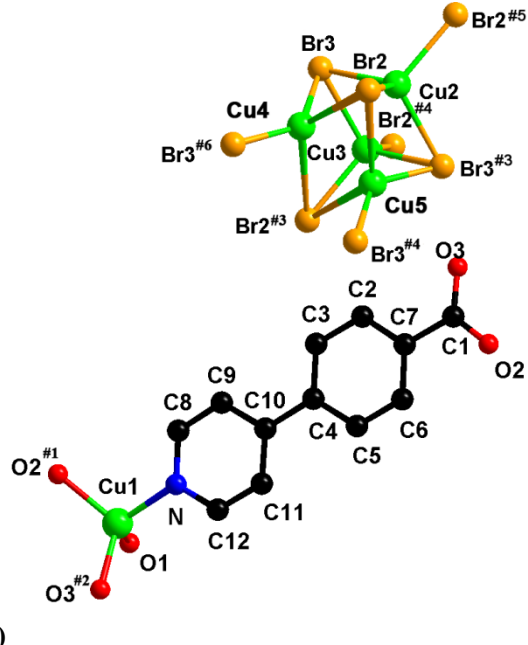


Fig. S1 a) The asymmetric unit of complex **1**. All H atoms are omitted for clarity. Symmetry codes: #1 $x-3/4, y-1/4, -z+1/2$; #2 $x-3/4, -y+1, z+1/4$; #3 $-x+9/4, y, -z+1/4$; #4 $x+1/2, -y+3/4, -z+1/4$; #5 $-x+11/4, -y+3/4, z$; #6 $x-1/2, -y+3/4, -z+1/4$. b) The 1-D chain-like guest based on the Cu_4Br_4 clusters shared by Cu_2Br_2 ring, in which four Cu atoms of the Cu_4Br_4 cluster possess tetrahedral geometry.

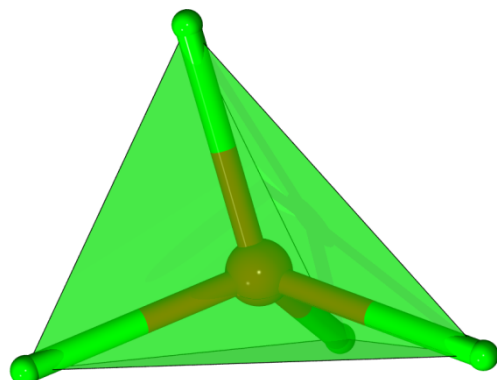


Fig. S2 The perspective view of the Cu_4O motif in the structure.

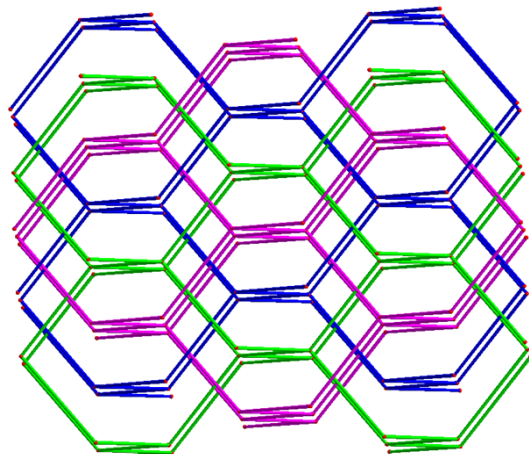


Fig. S3 The topological representation of the three-fold interpenetrating *dia* net of complex **1**.

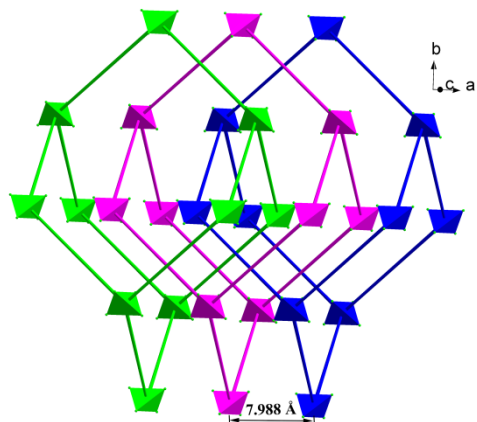


Fig. S4 The interlocked adamantane units of three independent diamond-like nets.

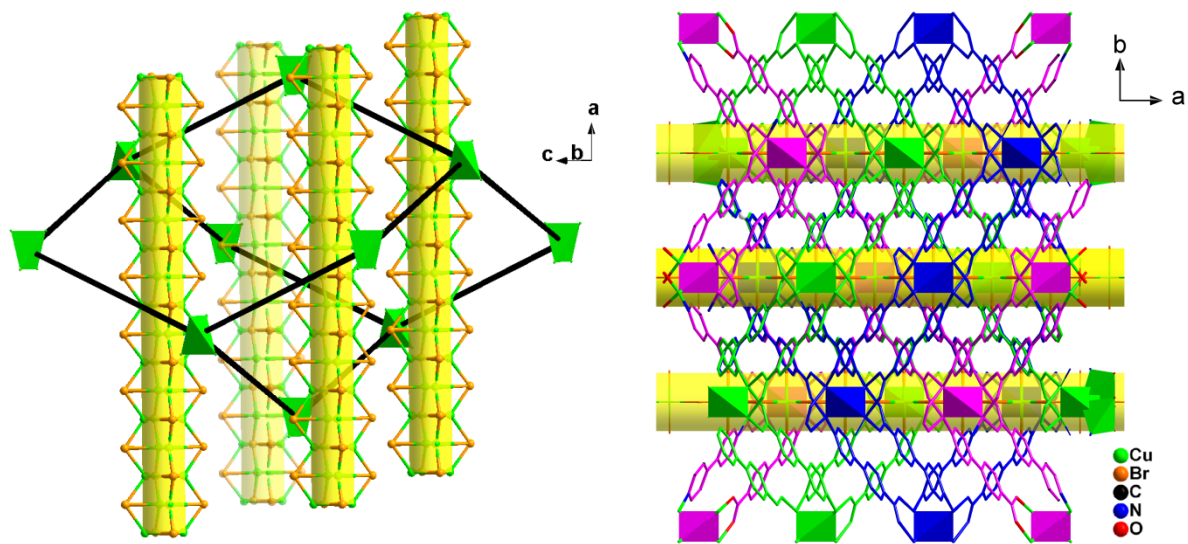


Fig. S5 The scheme representation of the 1D copper halide chains inset in an adamantane unit (left) and the overall side view of the host-guest compound (right).

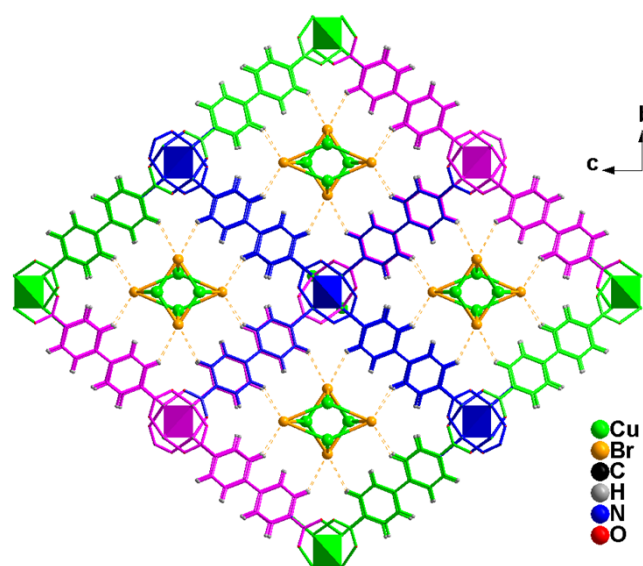


Fig. S6 The H-bonding interactions between host framework and guest chains.

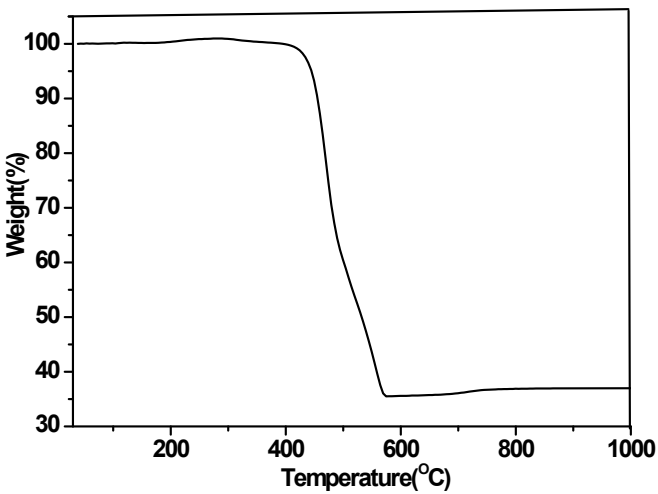


Fig. S7 The TGA curves of the compound **1**.

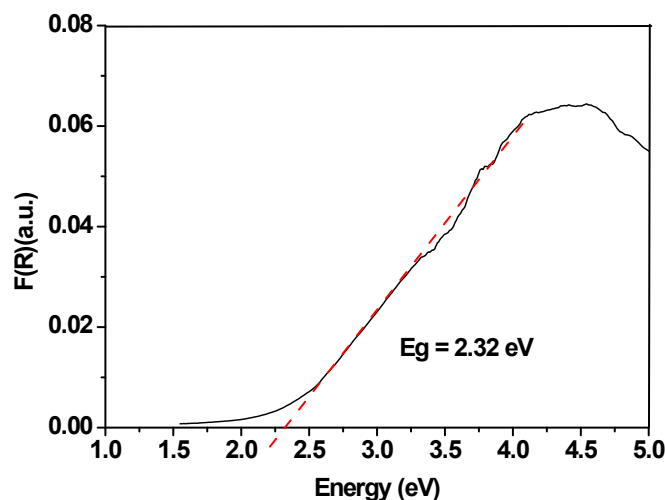


Fig. S8 The bands gap of the compound **1**.

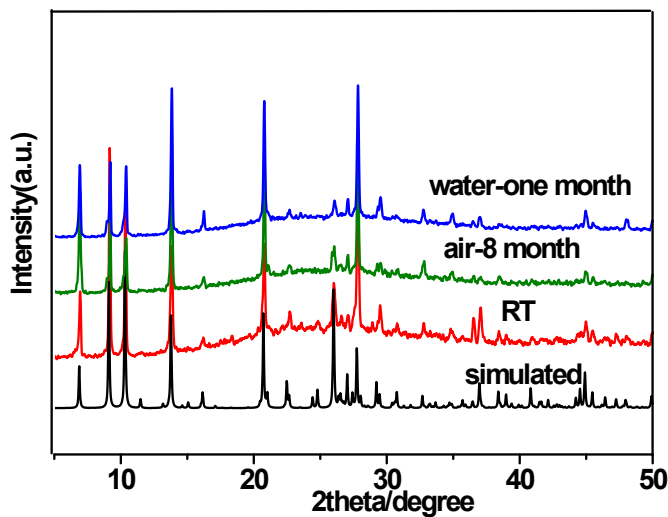


Fig. S9 PXRD patterns of **1** after being soaked in water and exposed in air for months.

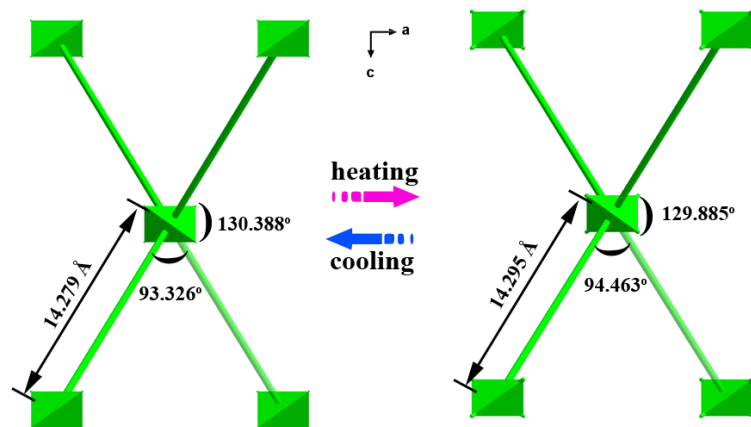


Fig. S10 Illustration of the “rhombus grid” showing the crystal structure transformation.

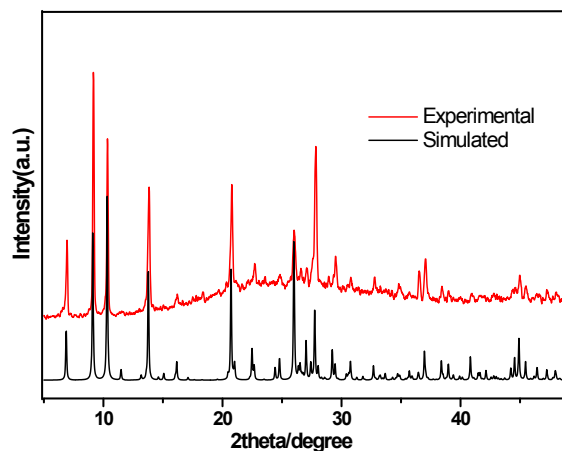


Fig. S11 The simulated and experimental PXRD patterns of compound **1**.

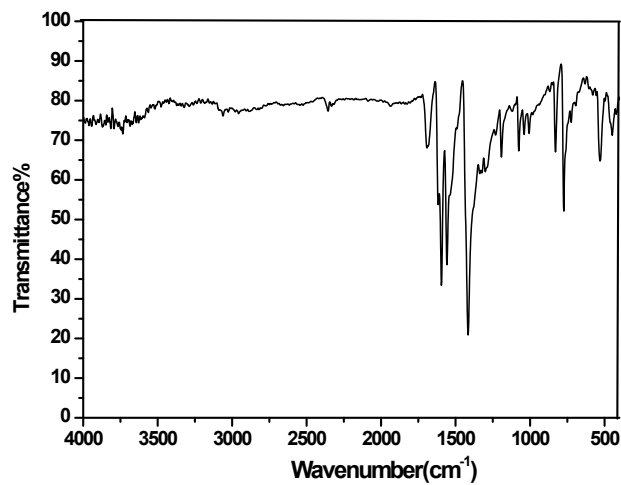


Fig. S12 The IR spectra of the complex **1**.

Supporting Tables:

Table S1 A summary of interpenetrating *dia* nets assembled by L ligands

Formula	interpenetrating degree	Ref.
Cd ^{II} Cu ^I ₂ L ₄	25	5
CdL ₂ ·H ₂ O	7	6
CuL·2H ₂ O	6	7
[Zn ₂ (μ-OH)L ₃]·EtOH	5	6
[Cd(L ₂) ₂](DMF)(H ₂ O) _{0.25}	4	8
[CoL ₂]·(MeOH) _{2.5} ·(H ₂ O)	4	9
[CoL ₂]·2DMF	4	10
Co(L ₂) ₂	4	11
[Cu ^{II} ₄ (μ ₄ -O)L ₄][Cu ^I ₆ Br ₈]	3	this work

Table S2. Bond valence sum (BVS) analysis^[a]

bond	r_0	r_{ij}	B	$S_{ij} = \exp[(r_0 - r_{ij})/B]$
Cu(1)-O(1)	1.679	1.968	0.37	0.458
Cu(1)-O(2)#1	1.679	1.943	0.37	0.490
Cu(1)-O(3)#2	1.679	1.948	0.37	0.483
Cu(1)-N	1.61	1.972	0.37	0.376
$V_{\text{Cu1}} = 1.81$				
Cu(2)-Br(2)	1.99	2.478	0.37	0.267
Cu(2)-Br(2)#3	1.99	2.478	0.37	0.267
Cu(2)-Br(3)#4	1.99	2.567	0.37	0.210
Cu(2)-Br(3)#5	1.99	2.567	0.37	0.210
$V_{\text{Cu2}} = 0.95$				
Cu(3)-Br(2)	1.99	2.494	0.37	0.256
Cu(3)-Br(2)#6	1.99	2.494	0.37	0.256
Cu(3)-Br(3)	1.99	2.542	0.37	0.225
Cu(3)-Br(3)#6	1.99	2.542	0.37	0.225
$V_{\text{Cu3}} = 0.96$				
Cu(4)-Br(2)(av)	1.99	3.1605	0.37	0.430
Cu(4)-Br(2)#6(av)	1.99	3.1605	0.37	0.430
Cu(4)-Br(3)(av)	1.99	2.302	0.37	0.042
Cu(4)-Br(3)#7(av)	1.99	2.302	0.37	0.042
$V_{\text{Cu4}} = 0.94$				

Cu(5)-Br(2)(av)	1.99	3.1339	0.37	0.045
Cu(5)-Br(2)#3(av)	1.99	3.1339	0.37	0.045
Cu(5)-Br(3)(av)	1.99	2.2923	0.37	0.442
Cu(5)-Br(3)#3(av)	1.99	2.2923	0.37	0.442

$$V_{Cu5} = 0.97$$

Symmetry codes: #1 $x-3/4, y-1/4, -z+1/2$; #2 $x-3/4, -y+1, z+1/4$; #3 $-x+9/4, y, -z+1/4$; #4 $x+1/2, -y+3/4, -z+1/4$; #5 $x+11/4, -y+3/4, z$; #6 $x-1/2, -y+3/4, -z+1/4$; #7 $-x+5/4, y, -z+1/4$.

[a] $V_i = \sum S_{ij} = \sum \exp[-(r_0 - r_{ij})/B]$, where r_0 is the length of a single bond, r_{ij} is the bond length between atoms i and j ; B is a constant, the “universal parameter” ~ 0.37 Å; S_{ij} is the valence of a bond between atoms i and j ; V_i is the sum of all bond valences of the bonds formed by a given atom i .

Table S3 Hydrogen bond lengths (Å) and bond angles (°) for compound **1**

Hydrogen bonds				
D-H···A	d(D-H)	d(H···A)	d(D···A)	∠(DHA)
C(5)-H(5A)···Br(2)#1	0.93	3.111(7)	3.826(8)	134.92
C(2)-H(2A)···Br(3)	0.93	3.247(2)	3.968(8)	136.07
Symmetry codes: #1 $-3/4+x, 1-y, 1/4+z$.				

Table S4 Temperature dependence of the unit-cell parameters of compound **1**.

T/K	a/Å	b/Å	c/Å	V/Å ³
100	7.990(2)	33.891(12)	39.171(10)	10606(7)
150	8.016(4)	34.031(15)	39.104(12)	10667(7)
200	8.029(3)	34.156(15)	39.004(11)	10697(7)
250	8.048(3)	34.246(15)	38.862(10)	10712(7)
300	8.081(5)	34.383(2)	38.714(17)	10757(10)
350	8.108(6)	34.426(3)	38.659(3)	10791(15)
400	8.122(5)	34.494(15)	38.558(10)	10803(11)
450	8.133(3)	34.586(11)	38.477(10)	10824(10)
500	8.147(5)	34.774(10)	38.424(12)	10877(12)

Table S5 Crystal data and structural refinement results

Complex	1	2
formula	$[Cu^{II}_4(\mu_4-O)L_4][Cu^{I}_6Br_8]$	$[Cu^{II}_4(\mu_4-O)L_4][Cu^{I}_6Br_8]$
formula weight	2083.46	2083.46
Temperature (K)	100(2)	298(2)
crystal system	orthorhombic	orthorhombic
Space group	<i>Fddd</i>	<i>Fddd</i>
<i>a</i> (Å)	7.98780(10)	8.072(2)
<i>b</i> (Å)	33.9352(6)	34.284(10)
<i>c</i> (Å)	39.1992(7)	38.825(11)

V (\AA^3)	10625.6(3)	10745(5)
Z	8	8
D_c (g cm^{-3})	2.605	2.576
μ (mm^{-1})	11.810	9.883
reflns collected	9896	19873
unique reflns	2692	3073
R_{int}	0.0227	0.0545
completeness	99.1%	99.1%
GOF on F^2	1.166	1.091
$R_1^{\text{a}}/\text{w}R_2^{\text{b}}[I > 2\sigma(I)]$	0.0606/0.1881	0.0616/0.1963
$R_1^{\text{a}}/\text{w}R_2^{\text{b}}(\text{all data})$	0.0616/0.1884	0.0685/0.2043

^a $R_1 = \sum ||F_o| - |F_c|| / \sum |F_o|$. ^b $\text{w}R_2 = \{\sum [w(F_o^2 - F_c^2)^2] / \sum [w(F_o^2)^2]\}^{1/2}$.

Table S6 Coordination bond lengths and angles of **1**

Bond lengths	100 K	298 K	Bond angles	100 K	298 K
Cu(1)-O(1)	1.9684(10)	1.9735(8)	O(2)#1-Cu(1)-O(3)#2	113.5(2)	114.8(3)
Cu(1)-O(2)#1	1.943(5)	1.942(5)	O(2)#1-Cu(1)-O(1)	102.84(15)	102.37(16)
Cu(1)-O(3)#2	1.948(6)	1.951(5)	O(3)#2-Cu(1)-O(1)	105.88(15)	105.97(16)
Cu(1)-N	1.972(6)	1.973(5)	O(2)#1-Cu(1)-N	106.2(2)	105.0(3)
Cu(2)-Br(2)	2.4776(16)	2.4755(19)	O(3)#2-Cu(1)-N	112.0(2)	112.1(2)
Cu(2)-Br(2)#3	2.4776(16)	2.4755(19)	N-Cu(1)-O(1)	116.27(17)	116.59(19)
Cu(2)-Br(3)#4	2.5666(16)	2.5914(18)	Br(2)-Cu(2)-Br(2)#3	110.95(12)	108.99(10)
Cu(2)-Br(3)#5	2.5666(16)	2.5914(18)	Br(2)-Cu(2)-Br(3)#4	108.75(3)	109.12(3)
Cu(3)-Br(2)	2.4935(17)	2.4872(19)	Br(2)-Cu(3)-Br(3)	108.74(3)	108.98(3)
Cu(3)-Br(2)#6	2.4935(17)	2.4872(19)	Br(2)#6-Cu(3)-Br(3)	109.33(3)	109.62(3)
Cu(3)-Br(3)	2.5421(16)	2.5672(18)	Br(3)#6-Cu(3)-Br(3)	113.69(11)	114.30(10)
Cu(3)-Br(3)#6	2.5421(16)	2.5672(18)	Br(3)-Cu(4)-Br(3)#7	121.6(2)	123.2(2)
Cu(4)-Br(2)(av)	3.1605(1)	3.1575(5)	Br(3)#5-Cu(4)-Br(2)	117.89(18)	116.9(2)
Cu(4)-Br(2)#6(av)	3.1605(1)	3.1575(5)	Br(3)-Cu(5)-Br(2)#4	116.9(2)	117.0(2)
Cu(4)-Br(3)(av)	2.302(1)	2.3072(5)	Br(3)#4-Cu(5)-Br(2)#4	117.1(2)	115.6(2)
Cu(4)-Br(3)#7(av)	2.302(1)	2.3072(5)			
Cu(5)-Br(2)(av)	3.1339(5)	3.1331(5)			
Cu(5)-Br(2)#3(av)	3.1339(5)	3.1331(5)			
Cu(5)-Br(3)(av)	2.2923(5)	2.3016(5)			
Cu(5)-Br(3)#3(av)	2.2923(5)	2.3016(5)			

Symmetry codes: #1 $x-3/4, y-1/4, -z+1/2$; #2 $x-3/4, -y+1, z+1/4$; #3 $-x+9/4, y, -z+1/4$; #4 $x+1/2, -y+3/4, -z+1/4$; #5 $-x+11/4, -y+3/4, z$; #6 $x-1/2, -y+3/4, -z+1/4$; #7 $-x+5/4, y, -z+1/4$.

References

- [1] W. W. Wendlandt, H. G. Hecht, *Reflectance Spectroscopy*, Interscience Publishers, New York, **1966**.
- [2] G. M. Sheldrick, *SHELXS97, Program for Crystal Structure Solution* (University of Göttingen, Göttingen, Germany, 1997).
- [3] G. M. Sheldrick, *SHELXL97, Program for Crystal Structure Refinement* (University of Göttingen, Göttingen, Germany, 1997). .
- [4] DIAMOND, in *Visual Crystal Structure Information System, version 3.2*, Crystal Impact: Bonn, Germany, **2004**.
- [5] Y. P. He, Y. X. Tan, J. Zhang, *CrystEngComm* **2012**, *14*, 6359-6361.
- [6] O. R. Evans, W. B. Lin, *Chem. Mater.* **2001**, *13*, 2705-2712.
- [7] T. B. Lu, R. L. Luck, *Inorg. Chim. Acta* **2003**, *351*, 345-355.
- [8] X. J. Zhou, B. Y. Li, G. H. Li, Q. Zhou, Z. Shi, S. H. Feng, *CrystEngComm* **2012**, *14*, 4664-4669.
- [9] G. Mehlana, G. Ramon, S. A. Bourne, *CrystEngComm* **2013**, *15*, 9521-9529.
- [10] M.-H. Zeng, Y.-X. Tan, Y.-P. He, Z. Yin, Q. Chen, M. Kurmoo, *Inorg. Chem.* **2013**, *52*, 2353-2360.
- [11] S. K. Elsaidi, M. H. Mohamed, L. Wojtas, A. Chanthapally, T. Pham, B. Space, J. J. Vittal, M. J. Zaworotko, *J. Am. Chem. Soc.* **2014**, *136*, 5072-5077.